Taylor & Francis
Taylor & Francis Group

Tribology - Materials, Surfaces & Interfaces

ISSN: 1751-5831 (Print) 1751-584X (Online) Journal homepage: https://www.tandfonline.com/loi/ytrb20

Influence of Ti, B and Sr on tribological properties of A356 alloy

D G Mallapur, K R Udupa & S A Kori

To cite this article: D G Mallapur, K R Udupa & S A Kori (2011) Influence of Ti, B and Sr on tribological properties of A356 alloy, Tribology - Materials, Surfaces & Interfaces, 5:1, 34-42, DOI: 10.1179/1751584X11Y.0000000001

To link to this article: https://doi.org/10.1179/1751584X11Y.0000000001

Published online: 12 Nov 2013.

Influence of Ti, B and Sr on tribological properties of A356 alloy

D. G. Mallapur*[1], K. R. Udupa[1] and S. A. Kori[2]

The wear behaviour of an A356 alloy has been investigated in this paper. To understand the wear behaviour of the materials, the experiments were carried out using a pin on disc testing machine at various combinations of normal pressure, sliding speed and sliding distances. Tribological results reveal that weight loss of A356 alloy increases with increasing normal pressure and decreases with increasing sliding speed. Also, the results at microlevel revealed a structural change from coarse columnar dendrites to fine equiaxed ones on the addition of grain refiner (Al and B) and furthermore, plate-like eutectic silicon to fine particles on addition of modifier (Sr). It is further noted in the present study that addition of modifier does not disturb the influence of grain refiner and *vice versa*. Abrasive wear mechanism was interrupted by the formation of microwelds and later by oxidation of the Al matrix.

Keywords: Grain refinement, Modification, Microstructure, Wear, A356 alloy

Introduction

Aluminium alloys have attractive physical and mechanical properties. They are lightweight, have low cost production, easy to machine and have good recycling possibilities (up to 95%).[1] Hypoeutectic Al–Si alloys (<10%Si) find a wide range of applications in marine, automobile and aircrafts where it is used for cylinder blocks, heads and other engine body castings. Hypoeutectic Al–Si alloys are used in many industrial applications because of their favourable strength to weight ratio and excellent castability.[2–4] Aluminium alloys A356, one of the categories of hypoeutectic Al–Si alloys, are mostly used to produce auto components because of a number of distinct benefits. Such benefits include low specific gravity, excellent castability, fluidity, high resistance to wear, reduced thermal expansion because of the presence of Si and adequate physical and mechanical properties at elevated temperatures.[5–9] A356 alloy contains ~50 vol.-% eutectic phase; hence, the final microstructure is largely determined by the mode of eutectic reaction. Eutectic silicon is present as coarse polyhedral particles and consequently the casting exhibits poor mechanical properties.[10] The chemical modifiers such as sodium and strontium are known to improve certain casting characteristics significantly. However, they have other undesirable effects.[10] Modification changes the eutectic silicon morphology, whereas grain refining reduces the size of the grain.[11] Grain refinement in aluminium alloys is usually achieved by inoculating the intrinsic additives, Ti or B added in the form of master alloys.[12–14] Extensive studies have been carried out on modification and grain refinement of Al–Si alloys in general and A356 alloy in particular. However, it is of immense interest to study the wear behaviour of A356 which are optimally treated for grain refinement and modification.

It is proposed elsewhere that maximum benefit in mechanical properties can be derived by the combined addition of two grain refiners and a single modifier. In order to develop an insight into the mechanism of wear process, it is intended here to assess the wear behaviour of Al–Si alloys which are treated with lone grain refiner or modifier and compare the properties with optimally derived ones through combined addition of two grain refiners and single modifier.

Experimental

In the present work, Al–3Ti and Al–3B master alloys were prepared by the reaction of potassium titanium fluoride (K_2TiF_6) and potassium borofluoride (KBF_4) salts with liquid Al in an induction furnace (2 kg, 4·5 kW, 50 cycles/s medium frequency induction furnace; Ceratherm International Pvt Ltd) with neutral refractory lining.[15] The furnace temperature was controlled to an accuracy of $\pm 5^{\circ}C$ using a digital temperature controller with a chromel–alumel thermocouple. The master alloys were prepared based on the results of previous work.[2] Once the molten Al reaches the required temperature, the halide salts weighed in required propositions were added to the melt after preheating at 150°C. The temperature of the melt at which salt addition was made is referred to as reaction temperature. A reaction temperature of 800°C was used for Al–3Ti and Al–3B master alloys, while the reaction time was kept constant at 60 min. After the completion of the reaction time, the unspent salt was degassed

[1]Research scholar, Department of Metallurgical and Materials Engineering, NITK, Surathkal, Karnataka, India
[2]Department of Mechanical Engineering, R&D Centre, Basaveshwar Engineering College, Bagalkot, Karnataka, India

*Corresponding author, email drmallapur@yahoo.com

Received 9 November 2010; accepted 6 January 2011
DOI 10.1179/1751584X11Y.0000000001

with commercial degasser, i.e. solid hexachloroethane (C_2Cl_6), to facilitate the removal of any gases present in the melt. After degassing, the melts were poured into cylindrical graphite mould (25 mm diameter and 250 mm height).

Master alloys are characterised by particle size analysis using image analyser, chemical analysis, XRD and SEM/EDX studies. Melting of the A356 alloy was carried out in a resistance furnace under a cover flux (45% NaCl + 45% KCl + 10% NaF) and the melt was held at 720°C. After degassing with solid C_2Cl_6, the indigenously developed master alloy chips (Al–3Ti and Al–3B) duly packed in an aluminium foil was added to the melt for grain refinement studies and for modification, Al–10Sr master alloy was used. The melt was stirred for 30 s with zircon coated steel rod after the addition of grain refiner and/or modifier, after which no further stirring was carried out. Melt were poured at an instant of '0' min and at the end of '5' min into cylindrical graphite mould. Three types of graphite moulds were used:

(i) top open cylindrical mould of dimension 25 mm diameter and 100 mm height for microstructure studies
(ii) split type graphite mould 12·5 mm diameter and 125 mm height for preparing wear sample of dimension 10 mm diameter × 32 mm length
(iii) split type graphite mould 12·5 mm diameter and 125 mm height for preparing tensile specimens of dimension 10 mm diameter × 50 mm length.

The '0' min refers to the melt without the addition of grain refiner and or modifier. Table 1 shows the modes of treatment given to the melt before pouring. The chemical compositions of the commercial purity Al (99·8%), commercial A356 alloy, indigenously developed master alloys (such as Al–3Ti and Al–3B) and commercially available master alloys such as (Al–10Sr) were assessed using atomic absorption spectrometer (VARIAN-AA240) and are shown in Tables 2 and 3. To evaluate the performance of Al–Si alloys under dry sliding conditions, wear tests were carried out according to ASTM G99 standards[16] using pin on disc wear testing machine, which is one of the frequently used test rigs.[17–20] Wear tests were carried out on A356 alloys using a pin on disc type testing machine (TR-20; DUCOM, Bangalore, India). Wear test specimens are rounded bars with flat surface having dimensions of 32 mm length × 10 mm diameter. The flat portion of 10 mm diameter of the test specimen is in contact with a rotating disc. The disc material is made up of En 32 steel (diameter 160 mm and 8 mm thickness) with chemical composition (Fe–0·14C–0·18Si–0·52Mn–0·015S–0·019P–0·13Ni–0·05Cr–0·06Mo) and heat treated to get a hardness value of HRc65.[21] The surface roughness of the disc varies from 0·02 to 0·06 μm. A constant 90 mm track diameter was used throughout the experimental work. The wear tests were carried out under various service conditions such as varying normal pressure, different sliding speeds and different sliding distances. The details of the experimental parameters are shown in Table 4. The weight loss measured in gram was continuously monitored and the frictional force generated on the specimen was measured in newtons by using a frictional force sensor. The wear test data such as weight loss and frictional force under various normal pressures, with different sliding speeds and at different sliding distances of these alloys, are recorded.

In the present study, the tribological properties of A356 alloy were studied without and with the addition of 0·65% of Al–3Ti of grain refiner, 0·60% of Al–3B grain refiner and 0·20% of Al–10Sr modifier, and combined addition of both grain refiner and modifier. Figure 1*a* shows the cylindrical graphite mould surrounded by fireclay bricks and Fig. 1*b* shows castings obtained from cylindrical graphite mould showing the sections selected for characterisation. The study on worn surface was carried out on the prepared wear test specimen of 32 mm length × 10 mm diameter, using a pin-on disc type machine with a track diameter of 90 mm, which remained constant throughout the experiment. Wear tests was carried out on A356 alloy using a pin on disc type testing machine (TR-20; DUCOM). A split type graphite mould (12·5 mm diameter and 125 mm height) for preparing wear specimens (10 mm diameter × 32 mm length) is shown in Fig. 1*d*.[21]

Results and discussion

Microstructural studies

Microstructural studies were carried out using SEM on the samples of A356 alloy, before and after the individual addition of 0·65% of Al–3Ti grain refiner, 0·60% of Al–3B grain refiner, 0·20% of Al–10Sr modifier and combined addition of 0·65% of Al–3Ti, 0·60% of Al–3B and 0·20% of Al–10Sr using SEM. Figures 2 shows the SEM images of A356 alloy before and after refinement and or modification. From Fig. 2*a*, it is clear that in the absence of grain refiner, A356 alloy shows coarse columnar α-Al dendritic structure and unmodified needle-/plate-like eutectic silicon. With the addition of 0·65% Al–3Ti master alloy, A356 alloy shows little response towards grain refinement with structural transition from coarse columnar dendritic structure to

Table 2 Chemical compositions of commercial purity Al and A356 alloy

Alloy composition	Composition/wt-%									
	Si	Cu	Mg	Fe	Mn	Zn	Pb	Sn	Ti	Al
Al	0·11	…	…	0·18	…	…	…	…	…	Bal.
A356	6·96	0·1	0·3	0·5	0·3	0·1	0·1	0·05	0·2	Bal.

Table 1 Details of A356 alloys prepared at 720°C (at '0' and '5' min holding time)

Alloy no.	Alloy composition	Addition level of master alloy/wt-%	Content of Ti, B and/or Sr
1	A356	…	…
2	A356 + Al–3Ti	0·65	0·02Ti
3	A356 + Al–3B	0·60	0·018B
4	A356 + Al–10Sr	0·20	0·02Sr
5	A356 + Al–3Ti + Al–3B + Al–10Sr	0·65, 0·60, 0·20	0·02Ti, 0·018B, 0·02Sr

fine equiaxed structure as shown in Fig. 2*b*. With the addition of 0·60% of Al–3B master alloy, the structure of A356 alloy changes from columnar to finer equiaxed α-Al dendrites compared to the addition of Al–3Ti grain refiner as clearly observed in Fig. 2*c*, while eutectic silicon remains unmodified as expected. This could be due to the presence of AlB_2 particles present in the Al–3B master alloy and these particles act as heterogeneous nucleating sites during solidification of α-Al. With the addition of A356 alloy to 0·20% of Al–10Sr master alloy, the plate-like eutectic Si is converted in to fine particles and α-Al dendrites remain as columnar dendritic structure only as clearly seen in Fig. 2*d*. However, Fig. 2*e* shows the simultaneous refinement (α-Al dendrites) and modification (eutectic Si) of A356 alloy due to the combined action of AlB_2 and Al_4Sr particles present in Al–3B grain refiner and Al–10Sr modifier respectively. Further, with the addition of 0·20% of Al–10Sr to A356 alloy, the plate-like eutectic Si is converted into fine particles and α-Al dendrites remain as columnar dendritic structure as clearly observed from Fig. 2*d*. The Al–10Sr modifier contains Al_4Sr intermetallics and these atoms are absorbed onto the growth steps of the solid/liquid interface. The mechanism of modification of eutectic Si by the addition of Sr is termed as impurity induced twinning.[9] However, Fig. 2*e* shows the simultaneous refinement (α-Al dendrites) and modification (eutectic Si) of A356 alloy due to the combined addition of grain refiner and modifier containing $(Al,Ti)B_2$ and Al_4Sr particles, which are responsible for changing the microstructure.

Wear studies

The tribological properties of A356 alloy mainly depend on the shape and size of the α-Al grains and the eutectic silicon morphology. Addition of grain refiners to A356 alloy converts predominantly columnar dendritic structure into fine equiaxed dendritic structure and addition of modifier changes plate-like eutectic Si into fine particles, which leads to the improvements in mechanical properties.[2] The improvements which are observed in the present study depend on the structural differences between the grain refined, modified and combined effect of grain refiner and modifier in A356 alloy. The improvements in the wear behaviour of A356 alloy with the addition of grain refiner and modifier under various normal pressures with constant sliding speed $v=1{\cdot}884\ m\ s^{-1}$ and at constant sliding distance $L=3400$ m have been studied. The effect of normal pressure on weight loss of A356 alloy under different normal pressures (0·13, 0·25, 0·38, 0·50 and 0·63 N mm^{-2}), with constant sliding distance (3400 m) and at constant sliding speed ($1{\cdot}88\ m\ s^{-1}$) is shown in Figs. 3 and 4. From Fig. 3, it is clear that, weight loss increases with increasing normal pressure in all the cases studied. However, the wear loss does not vary in a linear fashion; it increases with increasing rate to become almost constant at higher normal pressure. Further, it can be noted that microstructural variation does not play a major role in the change of wear loss with respect to normal pressure. Even though materials treated with two grain refiners and modifier show a better wear behaviour compared to other varieties of materials, the difference in value being small needs to be neglected. It is also clear from the figure that the combined addition of grain refiner and modifier to A356 alloys have resulted in minimum wear rate as compared to the individual addition of grain refiner and modifier and in untreated conditions. It is due to the Al_3Ti and AlB_2 particles present in grain refiner and Al_4Sr particles present in modifier, which changes the microstructure of the alloy from coarse dendrites to fine equiaxed dendrites due to heterogeneous nucleation and plate-/needle-like eutectic Si into fine particles due to the twinning effect. In the absence of grain refiner, A356 alloy shows a weight loss of 0·0598 g at a normal pressure of 0·63 N mm^{-2}. With the addition of 0·65% of Al–3Ti and 0·60% of Al–3B grain refiners and 0·20% of Al–10Sr modifier, the weight losses decrease to 0·0587, 0·0572 and 0·0564 g respectively. Similarly, with the combined addition of 0·65% of Al–3Ti and 0·60% of Al–3B grain refiners and 0·20% of Al–10Sr modifier to A356 alloy, the weight loss further decreases to 0·0553 g at identical conditions. The present results suggest that the combined addition of grain refiner and modifier leads to less wear rate when compared to individual addition of grain refiner and modifier, and supports the results macroscopy and microscopy studies. The profile of frictional force versus normal pressure as presented in Fig. 4 indicates definite change of slopes two points. It could be conceived that as pressure increases, silicon particle comes into bearing action reducing the frictional force. However, at higher normal pressures, silicon particles are scuffed away increasing the effective contact between α-aluminium matrix and steel baseplate, which increases the frictional force to a higher level. From the figure, it clearly

Table 3 Chemical compositions of various master alloys used in present work

	Composition/wt-%							
Alloy composition	Si	Cu	Mg	Fe	Mn	Zn	Pb	Sn
Al–3Ti	0·13	…	…	0·20	…	2·98		Bal.
Al–3B	0·14	…	…	0·16	…		2·83	Bal.
Al–10Sr	0·10	…	…	0·16	10·0	…	…	Bal.

Table 4 Varying service conditions

Sl no.	Parameters	Variables	Constants
1	Normal pressure/N mm^{-2}	0·13, 0·25, 0·38, 0·50 and 0·63	At constant sliding speed $v=1{\cdot}884\ m\ s^{-1}$ and at constant sliding distance $L=3400$ m of A356 alloy
2	Sliding speed/m s^{-1}	0·47, 0·94, 1·41, 1·88, 2·33 and 2·82	At constant normal pressure $P=0{\cdot}63$ N mm^{-2} and at constant sliding distance $L=3400$ m of A356 alloy
3	Sliding distance/m	850, 1700, 2540, 3400 and 4240	At constant normal pressure $P=0{\cdot}63$ N mm^{-2} and at constant sliding speed $v=1{\cdot}88\ m\ s^{-1}$ of A356 alloy

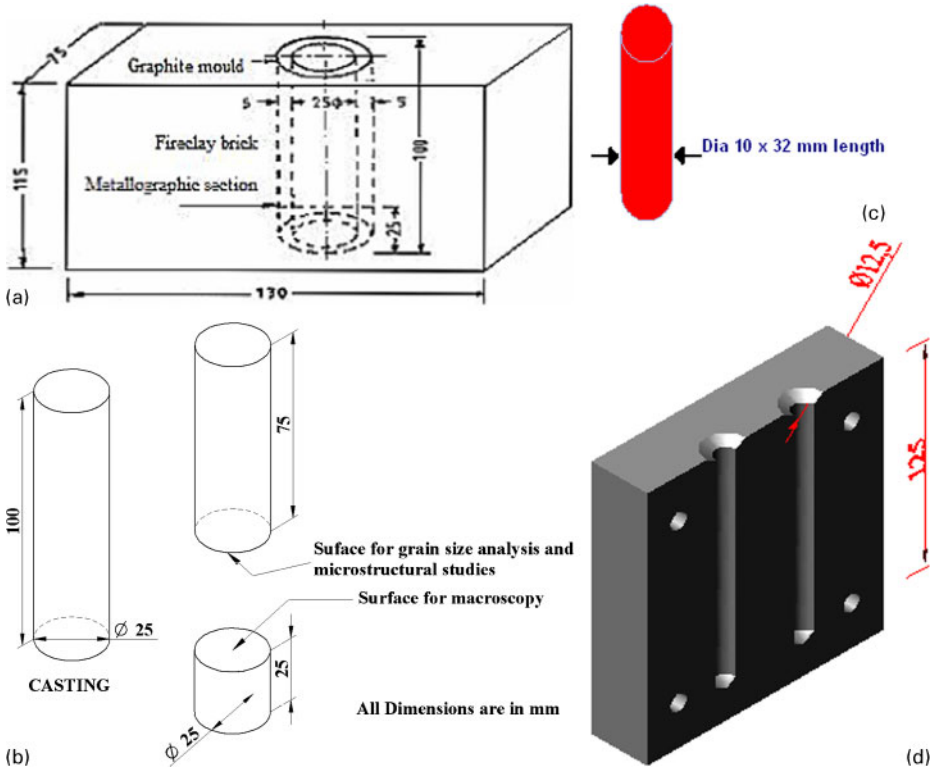

1 ***a*** **cylindrical graphite mould surrounded by fireclay bricks,** ***b*** **castings obtained from cylindrical graphite mould showing sections selected for characterisation,[2]** ***c*** **wear test specimen (10 mm diameter × 32 mm length) and** ***d*** **part of split type graphite mould (12·5 mm diameter and 125 mm height)[21]**

indicates that the frictional force increases with increasing normal pressure in almost all the cases studied of A356 alloy. In the present work, with the individual addition of 0·65% of Al–3Ti, 0·60% of Al–3B grain refiners and 0·20% of Al–10Sr modifier, and combined additions of 0·65% of Al–3Ti and 0·60% of Al–3B grain refiners and 0·20% of Al–10Sr modifier to A356 alloy, less frictional force is shown, as compared to the absence of grain refiner and modifier as clearly observed from Fig. 4. Such a decrease in the frictional force in A356 alloys could be due to the change in the microstructure from coarse to fine dendrites and plate-like eutectic Si into fine particles, which reduces the area of contact of eutectic silicon compared to the unmodified form. In addition, change in the microstructure leads to the toughness and strength of the alloy leading to lesser frictional force.

The effects of grain refinement and modification of A356 alloys on the weight loss and frictional force under different sliding speeds (0·47, 0·94, 1·41, 1·88, 2·35 and 2·82 m s^{-1}), with constant normal pressure 0·63 N mm^{-2} and at constant sliding distance 3400 m are shown Figs. 5 and 6. Profile presented in Fig. 5 shows the relation between weight loss and sliding distance. It can be inferred from the profile that in general weight loss gradually decreases as the sliding speed increases. It is clear from Fig. 5 that, with increasing sliding speed, there was a decrease in weight loss in the case of both grain refined/modified and without refined/modified A356 alloys. This is due to the fact that, at low sliding speeds, more time is available for the formation and growth of welds, which increases the force, which is required to shear off the microwelds, due to which the weight loss was higher. However, at higher speeds, there was less residential time for the growth of microwelds leading to lesser weight loss. In the absence of grain refiner, A356 alloy shows a weight loss and with the addition of 0·65% of Al–3Ti grain refiner, 0·60% of Al–3B grain refiner and 0·20% of Al–10Sr modifier, the weight loss decreases further. Similarly, with the combined addition of 0·65% of Al–3Ti grain refiner, 0·60% of Al–3B grain refiner and 0·20% of Al–10Sr modifier, the weight loss further decreases. The effects of grain refinement and modification of A356 alloys on frictional force under different sliding speeds with constant normal pressure and at constant sliding distance are shown in Fig. 6. It is clear from the profile that the frictional force increases with increasing sliding speed for materials without and with the addition of grain refiner and or modifier. However, with further increasing sliding speed, a decrease in the frictional force was observed. In addition, the frictional force is always lower in grain refined and modified alloys when compared to the untreated alloy. This is due to the fact that strength and hardness of the alloy improved with the addition of grain refiner and modifier when compared to the untreated A356 alloy. It is clear from Fig. 6 that with increasing sliding speed, there was an increase in frictional force in the case of both grain refined/modified and without refined/modified A356 alloys. This is due to the increase in the temperature in the wear specimen. As the temperature increases in the specimen, the intimate contact between the wearing pin and the rotating disc increases due to which the alloy becomes softer at the wearing surface. Further, it is observed that as the sliding speed increases, the frictional force decreases

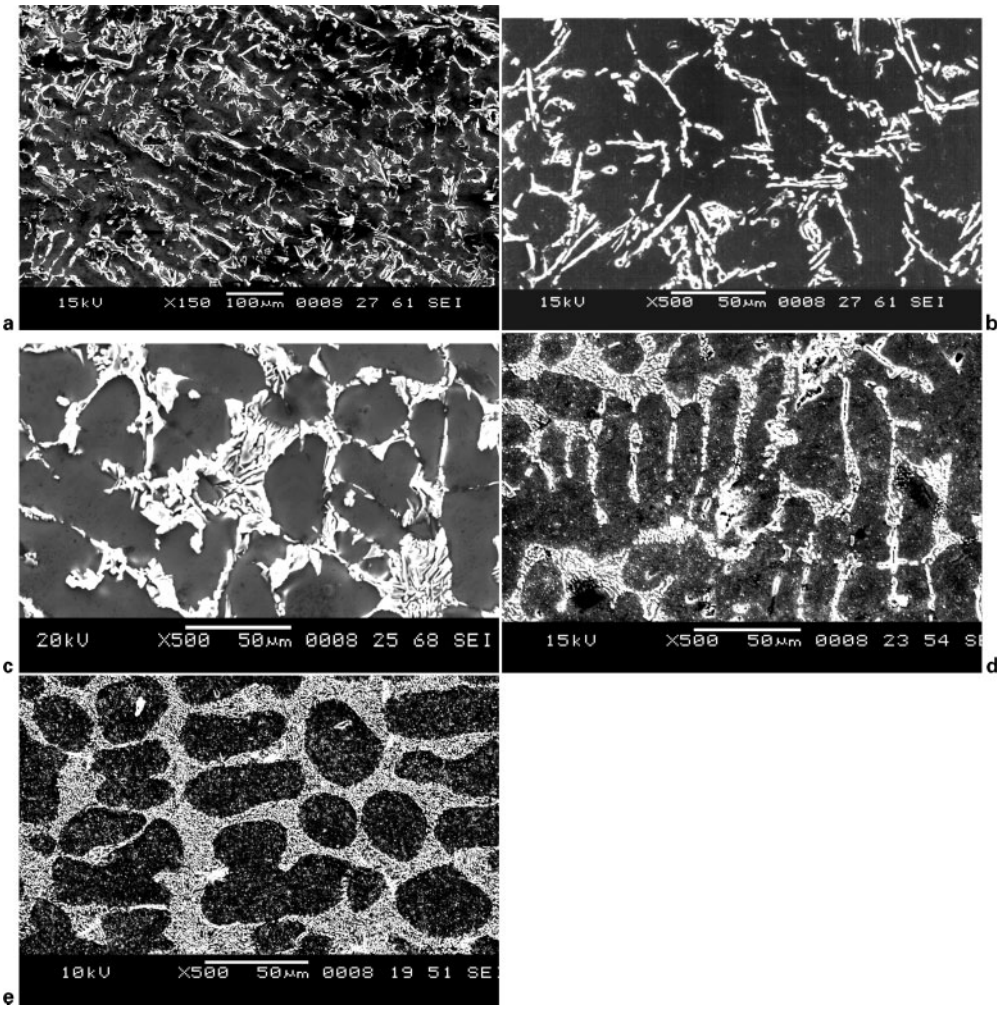

2 Photomicrographs (SEM) of A356 alloy *a* as cast alloy, *b* with 0·65% of Al–3Ti grain refiner, *c* with 0·60% of Al–3B grain refiner, *d* with 0·20% of Al–10Sr modifier and *e* combined addition of 0·65% Al–3Ti, 0·60% of Al–3B grain refiner and 0·20% of Al–10Sr modifier

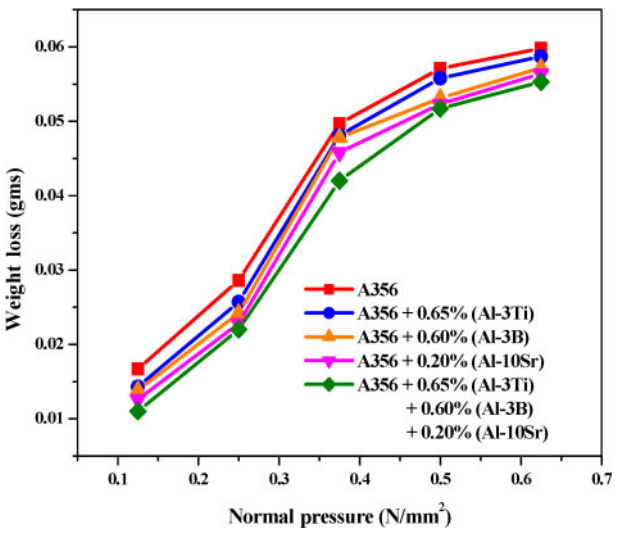

3 Effect of normal pressure on weight loss of A356 alloy: constant sliding speed v=1·88 m s^{-1} and at constant sliding distance L=3400 m

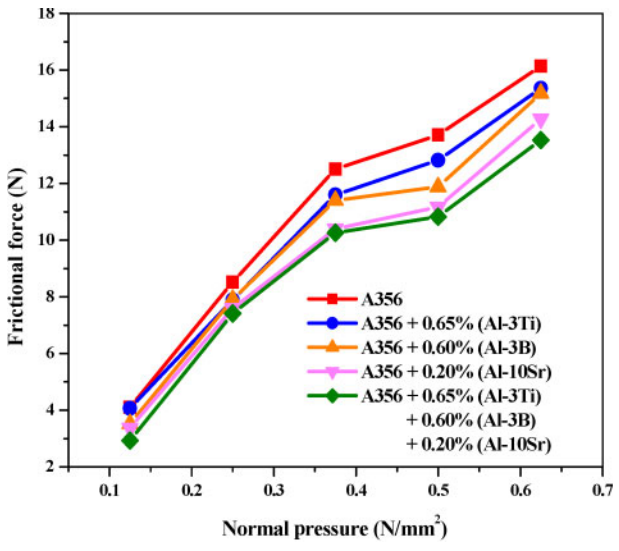

4 Effect of normal pressure on frictional force of A356 alloy: constant sliding speed v=1·88 m s^{-1} and at constant sliding distance L=3400 m

considerably, due to the increase in the frictional temperature which causes reducing shear stress at the wearing surface. With the addition of grain refiners, the toughness and hardness of the alloy increase and lead to less frictional force as compared to as cast alloy.

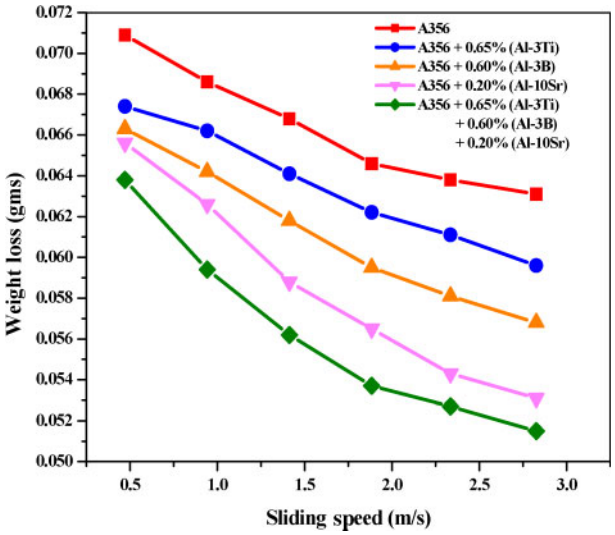

5 Effect of sliding speed on weight loss of A356 alloy: constant normal pressure P=0·63 N mm^{-2} and at constant sliding distance L=3400 m

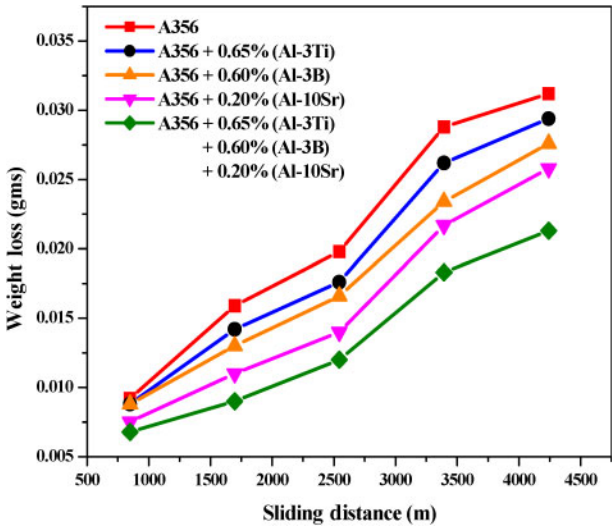

7 Effect of sliding distance on weight loss of A356 alloy: constant normal pressure P=0·63 N mm^{-2} and at constant sliding speed v=1·88 m s^{-1}

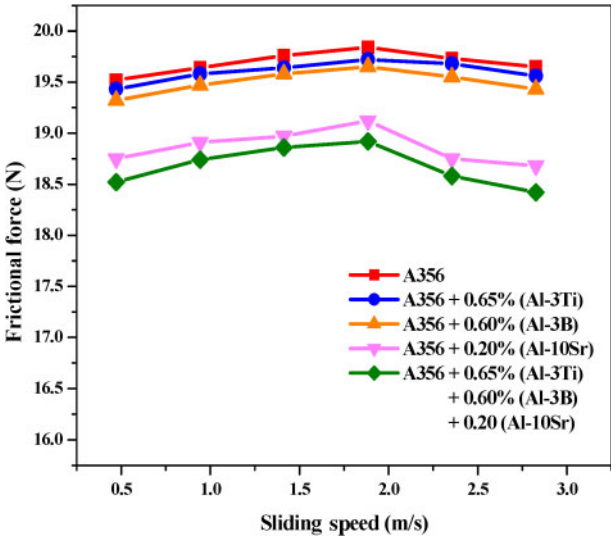

6 Effect of sliding speed on frictional force of A356 alloy: constant normal pressure P=0·63 N mm^{-2} and at constant sliding distance L=3400 m

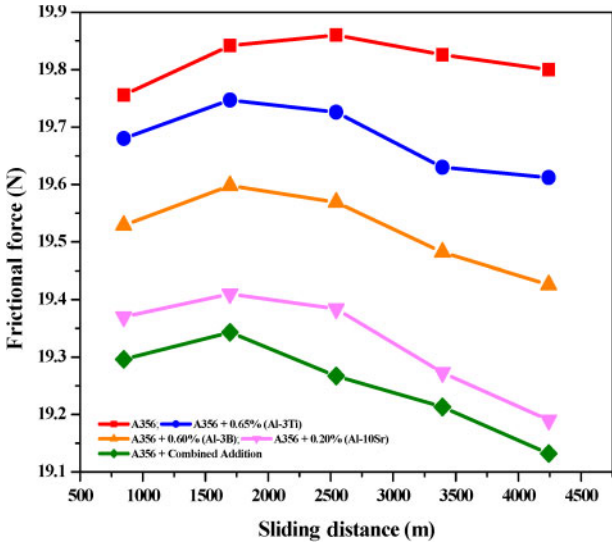

8 Effect of sliding distance on frictional force of A356 alloy: constant normal pressure P=0·63 N mm^{-2} and at constant sliding speed v=1·88 m s^{-1}

The effects of grain refinement and modification of A356 alloy on the weight loss and frictional force under different sliding distances (850, 1700, 2540, 3400 and 4240 m), with constant normal pressure (0·63 N mm^{-2}) and at constant sliding speed (1·88 m s^{-1}) are shown in Figs. 7 and 8. From the figures, it is clear that the weight loss increases with increasing sliding distance in all the cases studied. It is probably due to the fact that weight loss is directly proportional to the sliding distance. In the absence of grain refiner, A356 alloy shows weight losses of 0·00920 g at a lower sliding distance of 850 m and 0·0312 g at a higher sliding distance of 4240 m. With the addition of 0·65% of Al–3Ti grain refiner, the weight loss decreases. However, relatively lesser weight loss was observed with the individual addition of 0·60% of Al–3B grain refiner, 0·20% of Al–10Sr modifier and the combined addition of both to A356 alloy as clearly observed from Fig. 7. The reduction in weight loss of A356 alloy with the addition of grain refiner could be due to the fact that the addition of grain refiner leads to decrease in the grain size and results in the formation of more number of grain boundaries. Further reduction of in the weight loss with the addition of 0·20% of Al–10Sr modifier could be due to the conversion of sharp needle-/plate-like eutectic silicon into fine rounded particles, which reduces the stress concentration effect. Such structural changes reduce the crack nucleation tendency and results in improved wear resistance. From Fig. 8, it clearly indicates that the frictional force increases in the case of A356 with increasing sliding distance up to 2540 m and beyond that, frictional force decreases. It is probably due to the fact that friction is reduced due to the formation of oxide layer. The same trend is observed with the addition of grain refiners and also with the addition of modifiers, this could be due to the formation of oxide layer and addition of grain refiner leads to decrease in the grain size and results in the formation of more number of grain boundaries. Further reduction in

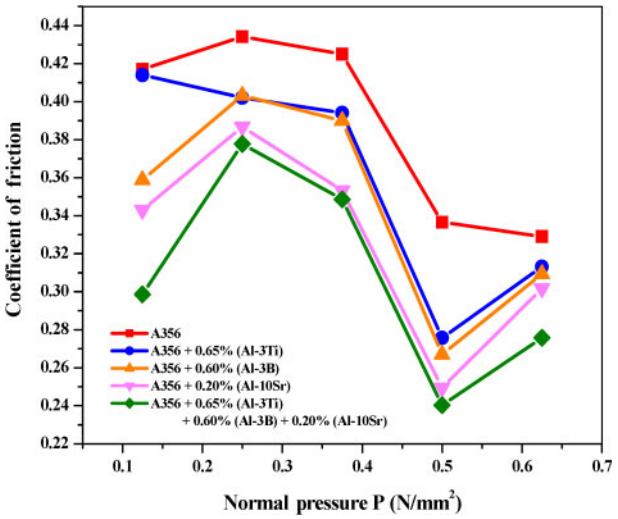

9 Effect of normal pressure on coefficient of friction of A356 alloy: constant sliding speed v=1·88 m s^{-1} and at normal pressure P=0·63 N mm^{-2}

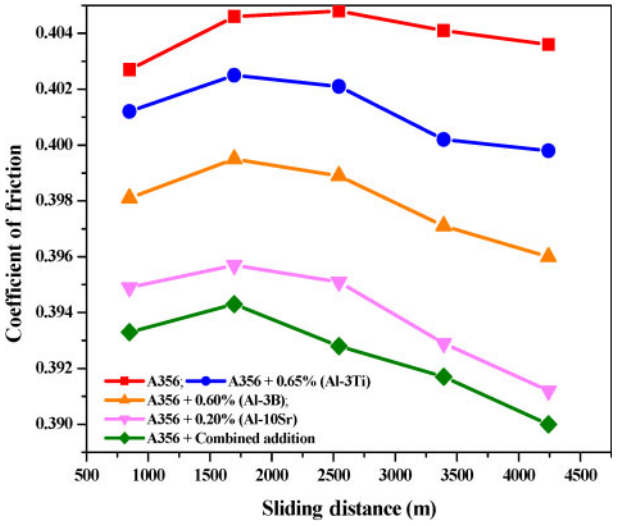

10 Effect of sliding distance on coefficient of friction of A356 alloy: constant sliding speed v=1·88 m s^{-1} and at normal pressure P=0·63 N mm^{-2}

the frictional force with the addition of 0·20% of Al–10Sr modifier could be due to the conversion of sharp needle-/plate-like eutectic silicon into fine rounded particles, which reduces the stress concentration effect. Such structural changes reduce the crack nucleation tendency and result in improved wear resistance.

From Fig. 8, it clearly indicates that the frictional force increases in the case of A356 with increasing sliding distance up to 2540 m and beyond that, frictional force decreases. It is probably due to the fact that friction is reduced due to the formation of oxide layer. The same trend is observed with the addition of grain refiners and also with the addition of modifiers, this could be due the formation of oxide layer and addition of grain refiner leads to decrease in the grain size and results in the formation of more number of grain boundaries. Further reduction in the frictional force with the addition of 0·20% of Al–10Sr modifier could be due to the conversion of sharp needle-/plate-like eutectic silicon into fine rounded particles, which reduces the stress concentration effect. Such structural changes reduce the crack nucleation tendency and result in improved wear resistance.

From Fig. 9, it is clearly observed that the coefficient of friction increases with increasing normal pressure 0·13–0·25 N mm^{-2}. However, as the normal pressure increases from 0·38 to 0·50 N mm^{-2}, a decrease in the coefficient of friction was observed at room temperature due to formation of oxide layer. It is also clear from the figure that the decrease in coefficient of friction in the case of A356 alloy is lesser as compared to individual and combined addition of grain refiners and modifier. Further, as the normal pressure increases from 0·50 to 0·63 N mm^{-2}, the coefficient of friction increases marginally due to the increases in the temperature. A similar trend is observed in Fig. 10.

Wear mechanisms

SEM studies of worn surfaces of A356 alloys were studied without and with the addition of 0·65% of Al–3Ti of grain refiner, 0·60% of Al–3B grain refiner and 0·20% of Al–10Sr modifier, and combined addition of both grain refiner and modifier. Each of the alloys was subjected to dry sliding wear test under constant conditions of 0·25 N mm^{-2} normal pressure, 1·884 m s^{-1} sliding speed and 3400 m sliding distance. Figure 11 shows the SEM images of the worn surfaces A356 alloy after the wear test. From Fig. 11*a*, it is clear that the worn surface of as cast A356 alloy consists of wide continuous parallel grooves. This indicates deeper penetration of the asperities of the harder disc and removal of more material from the contact surface of the wear pin, and hence, severe wear mode was observed in as cast A356 alloy. Figure also shows that, in the absence of grain refiner and modifier, there was a larger amount of fracture. This indicates deeper penetration of the asperities of the harder disc and removal of more material from the contact surface of the wear pin, and hence, severe wear mode was observed in as cast A356 alloy. The dislodging of the surfaces and removal of the material along the grain boundary lead to delaminative wear. However, the addition of 0·65% of Al–3Ti grain refiner and 0·60% of Al–3B grain refiner to A356 alloy resulted in reduced wear as clearly evident from Fig. 11*b* and *c*. With the addition of 0·60% of Al-3B grain refiner to A356 alloy, the worn surface shows fine grooves and with few small dimples when compared to the as cast alloy as seen in Fig. 11*c*. The reduction in wear of A356 alloy could be due to the fact that the addition of refiner leads to decrease in the grain size and formation of more number of grain boundaries. Such structural changes lead to the improvement in toughness and strength of the alloy owing to reduced wear rate. In the grain refined alloy, there was no crack formation on the worn surface and the wear mode observed was abrasive as clearly evident from Fig. 11*b* and *c*. The abrasive wear occurs because of the sliding of hard disc against soft pin surface. The disc digs in to the pin surface and plows a series of continuous parallel grooves (two-body wear). Abrasive wear also occurs when hard silicon particles are introduced between the two sliding surfaces. Similarly, Fig. 11*d* shows the worn surface of modified A356 alloy. From the figure, it is clear that the worn surface consists of a compacted oxide layer and a few discontinuous abrasive grooves, indicating that both oxidative and three-body abrasive

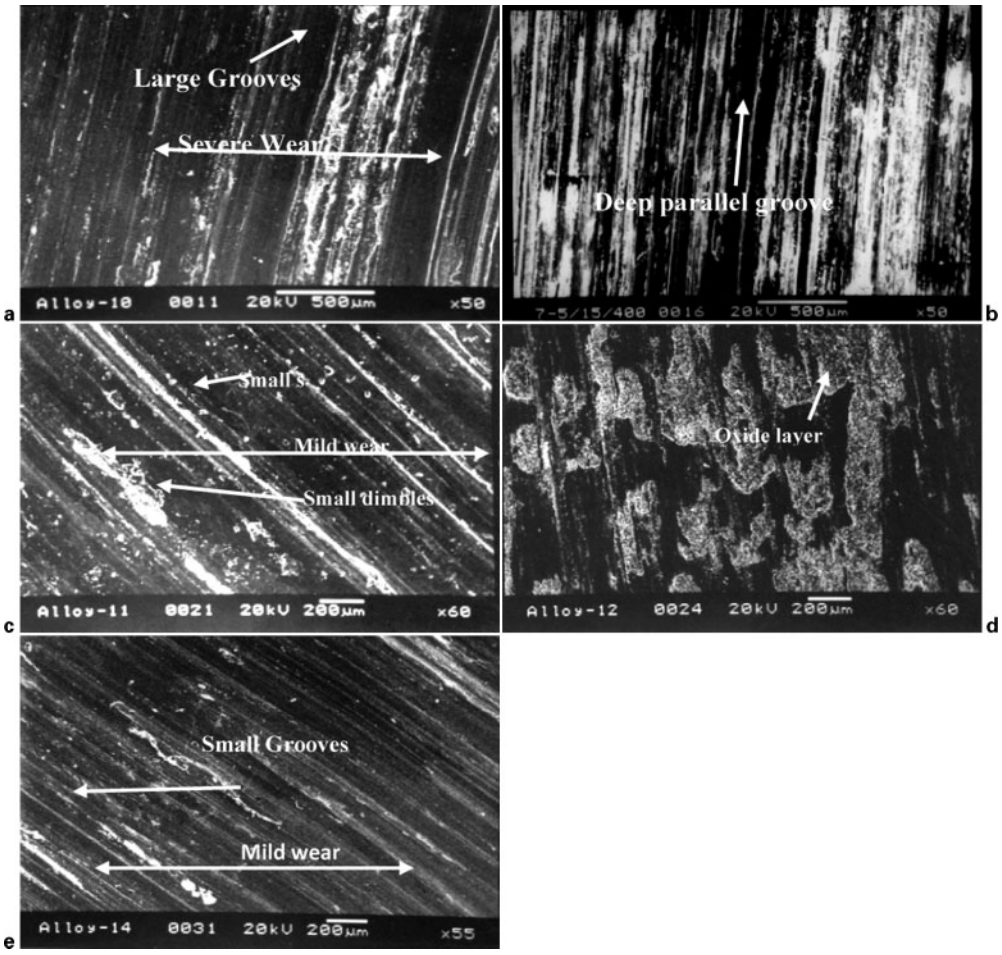

11 Photomicrographs (SEM) of worn surface of A356 alloy *a* without addition of grain refiner/modifier, *b* with addition of 0·65% of Al–3Ti grain refiner, *c* with addition of 0·60% of Al–3B grain refiner, *d* with addition of 0·20% of Al–10Sr modifier and *e* with combined addition of 0·65% Al–3Ti, 0·60% of Al–3B grain refiner and 0·20% of Al–10Sr modifier

wears were operated in the case of modified A356 alloy and also further reduction in the crack formation was observed with the addition of 0·20% of Al–10Sr modifier to A356 alloy. Modification of A356 alloy changes the microstructure from plate-/needle-like eutectic Si to fine rounded particles. The change in the morphology of Si particle reduces stress concentration and increases the binding of silicon crystals. Figure 11*e* shows the worn surface of A356 alloy when it was simultaneously treated with grain refiner and modifier. Numerous long and smooth grooves were observed on the worn surface indicating mild wear when compared to the alloy individually treated with grain refiner and modifier and in untreated conditions.

Conclusion

1. Wear behaviour of A356 Al–Si alloys is influenced by microstructural features of α-Al matrix and eutectic Si dispersed as second phase particle.

2. The wear mechanism changes from one mode to another with a change in pressure, velocity and distance.

3. Abrasive wear mechanism was interrupted by the formation of microwelds and later by oxidation of the Al matrix.

4. Scuffing of the Si, which depends upon the morphology, plays an important role.

5. Elements of delaminative wear mechanism were noted.

References

1. http://www.eaa.net.
2. S. A. Kori: 'Studies on the grain refinement and modification of some hypoeutectic and eutectic Al-Si alloys', PhD thesis, IIT Kharagpur, Kharagpur, India, 2000.
3. L. F. Mondlofo: 'Aluminium alloys – structure and properties', 249–250; 1976, London, Butterworths.
4. ASM International: 'ASM handbook', Vol. 2, 'Properties and selection: nonferrous alloys and special- purpose materials'; 1990, Materials Park, OH, ASM International.
5. D. K. Dwivedi: 'Wear behaviour of cast hypereutectic aluminium silicon alloys', *Mater. Des.*, 2006, **27**, 610–616.
6. J. R. Davis: 'Aluminum and aluminum alloys', ASM specialty handbook; 1993, Materials Park, OH, ASM International.
7. J. E. Gruzleski and B. M. Closset: 'The treatment of liquid aluminum–silicon alloys'; 1990, Des Plaines, IL, American Foundry Men's Society, Inc.
8. O. Madelaine-Dupuich and J. Stolarz: 'Fatigue of eutectic Al–Si alloys', *Mater. Sci. Forum*, 1996, **1343**, 217–222.
9. Z. Ma: 'Effect of iron-intermetallics and porosity on tensile and impact properties of Al–Si–Cu and Al–Si–Mg cast alloys', PhD thesis, Universite' du Que'bec a' Chicoutimi, Chicoutimi, Que., Canada, 2002.
10. A. G. A. Pelayo and A. M. Irisarri: *Mater. Sci. Technol.*, 2001, **17**, 446.
11. A. Thirugnanam, K. Sukumaran, K. Raghukandan, U. T. S. Pillai and B. C. Pai: 'Microstructural aspects and fracture behavior of A356/357 alloys – an overview', *Trans. Indian Inst. Met.*, 2005, **58**, (5), 777–787.
12. M. Johnsson and L. Backerud: 'Nucleus in grain refined Al after addition of Ti and B-containing master alloys', *Z. Metallkd*, 1992, **83**, (11), 774–780.
13. J. Huang, J. G. Conley and P. Callau: 'Alternative methods for porosity prediction in aluminium alloys', *SAE Techn. Pap.*, 1998, no. 980387.

14. A. L. Greer, A. M. Bunn, A. Tronche, P. V. Evans and D. J. Bristow: 'Modelling of inoculation of metallic melts: application to grain refinement of aluminium by Al–Ti–B', *Acta Mater.*, 2000, **48**, (11), 2823–2835.
15. V. Auradi: 'Development of Al–Ti, Al–B and Al–Ti–B master alloys for grain refinement of Al–Si alloys', PhD thesis, VTU Belgaum, Belgaum, India, 2006.
16. 'Standard test methods for wear testing with a pin-on-disc apparatus', G 99-90, ASTM, Philadelphia. PA, USA, 2009.
17. V. R. Kabadi: 'Studies on wear characteristics of plain carbon hypo-eutectoid and eutectoid steels', PhD thesis, IIT Kharagpur, Kharagpur, India, 2001.
18. N. Saheb, T. Laoui, A. R. Daud, M. Harun, S. Radiman and R. Yahaya: 'Influence of Ti addition on wear properties of Al–Si eutectic alloys', *Wear*, 2001, **249**, 656–662.
19. F. Wang, Y. J. Ma, Z. Y. Zhang, X. H. Cui and Y. S. Jin: 'A comparison of the sliding wear behavior of hypereutectic Al–Si alloy prepared by spray-deposition and conventional casting methods', *Wear*, 2004, **256**, 342–345.
20. R. Dasgupta and S. K. Bose: 'Effect of copper on the tribological properties of Al–Si base alloys', *J. Mater. Sci. Lett.*, 1995, **14**, 1661–1663.
21. T. M. Chandrashekharaiah: 'Studies on sliding wear behaviour of grain refined and modified hypoeutectic, eutectic and hypereutectic Al–Si alloys', PhD thesis, VTU Belgaum, Belgaum, India, 2007.